pagepress

Journal of Limnology

Journal of Limnology 2026; 85:2272
doi:10.4081/jlimnol.2026.2272

Millennial reconstruction of organic carbon burial and n-alkane-based source identification in Sayram Lake, Xinjiang, China

Wen Liu,[1,2,3] Jingyu Wang,[1,2,3] Yanli Guo,[1,2,3] Yizhen Li,[1,2,3] Tao Zeng,[1,2,3] Long Ma[1,2,3*]

[1]State Key Laboratory of Ecological Safety and Sustainable Development in Arid Lands, Xinjiang Institute of Ecology and Geography, Chinese Academy of Sciences, Urumqi; [2]Research Center for Ecology and Environment of Central Asia, Chinese Academy of Sciences, Urumqi; [3]University of Chinese Academy of Sciences, Beijing, China

Abstract

Organic carbon burial in lake sediments plays a crucial role in understanding the terrestrial carbon cycle. Sayram Lake (Xinjiang, China), located in the Tianshan Mountains of arid Central Asia, provides a unique opportunity to investigate the mechanisms governing organic carbon burial in deep lakes over the past millennia. With the source apportionment based on n-alkanes, the carbon burial pattern in the Tianshan Mountains over the past millennium was reconstructed using an integrated framework of Bayesian change-point detection and wavelet analysis. The organic carbon burial rate (OCBR) in Sayram Lake was characterized by the coexistence of periodicity and stages, with a significant power peak within the 40-90-year period range and the strongest signal occurring at approximately the 60-year period. Sediment grain size played a relatively minor role in the carbon burial process in Sayram Lake. The OCBR has been at a low level and has shown a decreasing trend since the Little Ice Age, which differs significantly from the trends observed in lakes within global inland basins. The influence of lake environmental system evolution and climate change on organic carbon burial was assessed using regional climate change datasets, which provided new data and insights into the mechanisms governing carbon burial in deep-water lakes within arid mountain ecosystems.

Key words: source apportionment; organic carbon burial; deep-lake sediments; millennial variations; Arid Central Asia.

Correspondence to: malong@ms.xjb.ac.cn

Introduction

Research on the carbon cycle is of significant scientific importance for enhancing our understanding of the functioning mechanisms of the Earth's system, addressing global environmental changes, and ensuring sustainable development of human society (Falkowski *et al.*, 2000). Lakes are key components of terrestrial ecosystems and constitute a significant carbon pool (Bar-On *et al.*, 2025). Inland waters bury carbon more efficiently than oceans because a higher fraction of sedimented organic carbon (OC) escapes mineralization and remains in sediments (Mendonça *et al.*, 2017). Lake carbon reservoirs play a crucial role in preserving the global carbon balance and alleviating the impacts of climate change (Tranvik *et al.*, 2009).

Understanding the driving mechanisms of past carbon burial holds significant scientific value for comprehending the multi-scale functioning of the Earth system (Bradley *et al.*, 2003; Jones *et al.*, 2001) and helps improve predictions of carbon pool changes under future global-change scenarios (Hülse *et al.*, 2017; Lan *et al.*, 2020b; Shi *et al.*, 2021). The burial of organic carbon in lakes has become a key area of research (Luo *et al.*, 2025; Quanliang *et al.*, 2024; Zhou *et al.*, 2025a; Zhou *et al.*, 2025b). Global carbon burial in lakes has significantly increased, with the carbon burial rate in lakes within tropical forests and grassland biomes quadrupling over the past century (Anderson *et al.*, 2020). Numerous studies have explored carbon sequestration in arid regions (Einsele *et al.*, 2001; Fang *et al.*, 2023; Lan *et al.*, 2015; Stallard, 1998; Xu *et al.*, 2013; Zhang *et al.*, 2017), with a particular focus on large shallow plain lakes in arid areas of Central Asia (Feng *et al.*, 2021; Liu *et al.*, 2021; Xie *et al.*, 2015; Yu *et al.*, 2015). However, marked heterogeneity in the rates of organic carbon burial has been observed across diverse geographical regions (Mendonça *et al.*, 2017), and there is a lack of research on deep mountain lakes in arid Central Asia. This research gap constrains the accurate global assessment of carbon burial magnitudes and the holistic identification of factors influencing organic carbon preservation.

Research on Sayram Lake spans multiple disciplines and has significantly advanced our understanding of past environmental and climatic changes. For instance, grain-size data have revealed aeolian activity history over the past century (Ma *et al.*, 2015), whereas multi-proxy analyses have reconstructed regional environmental and lake dynamics over the last 200 years (Liu *et al.*, 2014). Paleoclimate studies span multiple timescales, including Holocene vegetation evolution (Jiang *et al.*, 2013), climatic events since the last glacial period (Jiang *et al.*, 2019), a continuous increase in Holocene precipitation in northwestern China inferred from black carbon $\delta^{13}C$ records (Jiang *et al.*, 2020), and abrupt cooling in Central Asia since the early Little Ice Age, as indicated by alkenone

proxies (Yao *et al.*, 2020). Beyond climate reconstruction, geochemical investigations have traced the history and sources of heavy metal pollution over the past 200 years (Zeng *et al.*, 2014), providing novel insights into recent human activities through sedimentary records of Polycyclic Aromatic Hydrocarbons (Shen *et al.*, 2018). Sediment mineralogy has further revealed the nonbiological origin of Holocene primary dolomite in the lake (Cheng *et al.*, 2021). Microbiological studies have characterized bacterial community composition (Shao *et al.*, 2023b; Shao *et al.*, 2023c), compared planktonic and sedimentary bacterial diversity in summer (Fang *et al.*, 2015), examined the presence and diversity of Atribacteria in sediment cores (Shao *et al.*, 2023a), and reported shifts in bacterial communities within lake ecosystems (Hu *et al.*, 2025). Collectively, these studies demonstrate the utility of Sayram Lake sediments as valuable archives of both natural environmental change and anthropogenic impact.

To address the research gap regarding carbon burial in alpine lakes and its influencing factors in the arid regions of Central Asia, this study established a high-resolution sequence of organic carbon burial fluxes in the deep-lake sediments of Sayram Lake over the past millennium, using an age-depth model constrained by radiocarbon dating. Based on this reconstruction, the temporal variability of organic carbon burial will be systematically analyzed using an integrated framework combining Bayesian change-point detection and wavelet analysis. To further elucidate the underlying driving mechanisms, this study will employ n-alkane-based source apportionment to identify the origins of sedimentary organic matter and integrated regional paleoclimate records to examine how lake environmental system evolution and climatic forcing influence organic carbon burial dynamics. Collectively, these results provide new data and mechanistic insights into the carbon burial processes of deep-water lakes in mountain ecosystems within arid regions.

METHODS

Geographical setting

The Tianshan Mountains, often referred to as the Water Tower of Central Asia (Fan *et al.*, 2020; He *et al.*, 2015), stretch over 2,500 km from east to west and are located in the heart of the Eurasian continent. They are one of the major areas of modern glacier distribution in China (Cai *et al.*, 2021; Wang *et al.*, 2011). Sayram Lake is located in a intermontane depression basin in the western Tianshan Mountains (Fig. 1).

According to a previous study (Harris *et al.*, 2020), the Sayram Lake Basin experiences a temperate continental climate, with an average temperature of 1.1°C, annual evaporation of 550 mm, and precipitation of 385.9 mm. The basin is subject to the influence of the westerly wind belt, with westerly winds constantly present in the lake area throughout the year. Rainwater and groundwater are primary sources of lake water replenishment. The Sayram Lake Basin is characterized by a pronounced vertical zonation. The alpine ice and snow belt, which dominates at elevations above 3800 m, transitions into a sparse alpine vegetation belt, which gradually shifts to an alpine meadow belt at elevations ranging from 3800 to 2800 m. At lower elevations (2800-2400 m), the landscape features subalpine grassland meadows, whereas at lower elevations (2400-2150 m), the vegetation transitions to mountain meadow grasslands. Finally, the lakeshore area is characterized by desert grassland. Sayram Lake is 28 km in length from east to west and 21 km in width from north to south. Its surface area is 462 km^2 and its catchment area is 1,408 km^2 (Wu *et al.*, 2014). The maximum of water depth was 99 m, and the total storage capacity was 261 × 10^8 m^3(Wu *et al.*, 2014). The freezing period typically occurs in October, and the thawing process commences in the first half of May of the following year.

Sampling and laboratory analysis

According to a bathymetric survey (Wu *et al.*, 2014), a location characterized by a relatively stable sedimentary environment and a water depth of 90 m was identified as the site for sediment core collection. During the ice-covered period in February 2023, a sediment core (44°39′18.06″N, 81°06′34.76″ E, SLM, 66 cm) was collected from the center of Sayram Lake using a Uwitec gravity corer (UWITEC Ltd., Mondsee, Austria) equipped with a sampling tube with a diameter of 60 mm (Fig. 2a).

The SLM core samples were collected at 1.0 cm intervals and stored in plastic bags at 4°C for subsequent analysis. The dry density of the samples was calculated after drying at a low temperature. Bulk organic carbon from the columnar sediments was dated using ^{14}C analysis at the Beta AMS^{14}C Laboratory in the United States. Because no plant debris or remains were found in the core, bulk organic carbon samples were selected for ^{14}C dating. All AMS^{14}C ages were calibrated using the INTCAL20 database with rbacon (https://CRAN.R-project.org/package=rbacon).

Subsamples of dried sediment were analyzed for ^{210}Pb, ^{226}Ra, and ^{137}Cs using direct gamma spectrometry with an Ortec HPGe GWL series, a well-type coaxial, low-background, and intrinsic germanium detector (Wu *et al*., 2004). Preparation, treatment, and geochemical analyses were conducted at the State Key Laboratory of Lake Science and Environment, Chinese Academy of Sciences.

The sediment particle size index was measured using a BETTERSIZER (BT-9300SE) laser grain size analyzer. The measurement range of the instrument was 0.1-1000 μm, and the accuracy and repeatability errors were ≤1% (national standard D50 deviation). The specific experimental procedure was as follows: 0.2 g unground sediment samples were weighed and transferred to a beaker. Subsequently, 10 mL of hydrogen peroxide (H_2O_2) at a concentration of 10% was added. The beaker was then heated to eliminate the organic matter. To eliminate carbonate impurities, 10 mL of 10% hydrochloric acid (HCl) was added. This step was completed after heating the mixture in the absence of bubbles. After the reaction was complete, deionized water was added to the beaker, which was left undisturbed for 12 h. The clear upper layer of the liquid was subsequently removed, and 10 mL of a 0.05 mol L^{-1} sodium hexametaphosphate ($(NaPO_3)_6$) solution was added to it. The mixture was then subjected to ultrasonic vibration for 10-15 min to ensure complete dissolution. Finally, the apparatus was placed in a machine for particle size testing. The experiment was repeated thrice for each specimen, and the results were calculated as the mean of three replicates.

TOC and TN were analyzed at the Institute of Earth Environment, Chinese Academy of Sciences. The samples were dried, ground, and passed through a 200-mesh sieve. Measurements were conducted using a soil TOC cube elemental analyzer (Elementar Analysensysteme GmbH, Langenselbold, Germany) in accordance with the international standard method (DIN 19539). A quality control method was employed to assess the blank background value and standard samples of loess and calcium carbonate, with a detection limit of 20 ppm and a standard deviation of less than 0.1%. The molar ratio of carbon to nitrogen (C:N) was determined from the total organic carbon (TOC) and total nitrogen (TN) content.

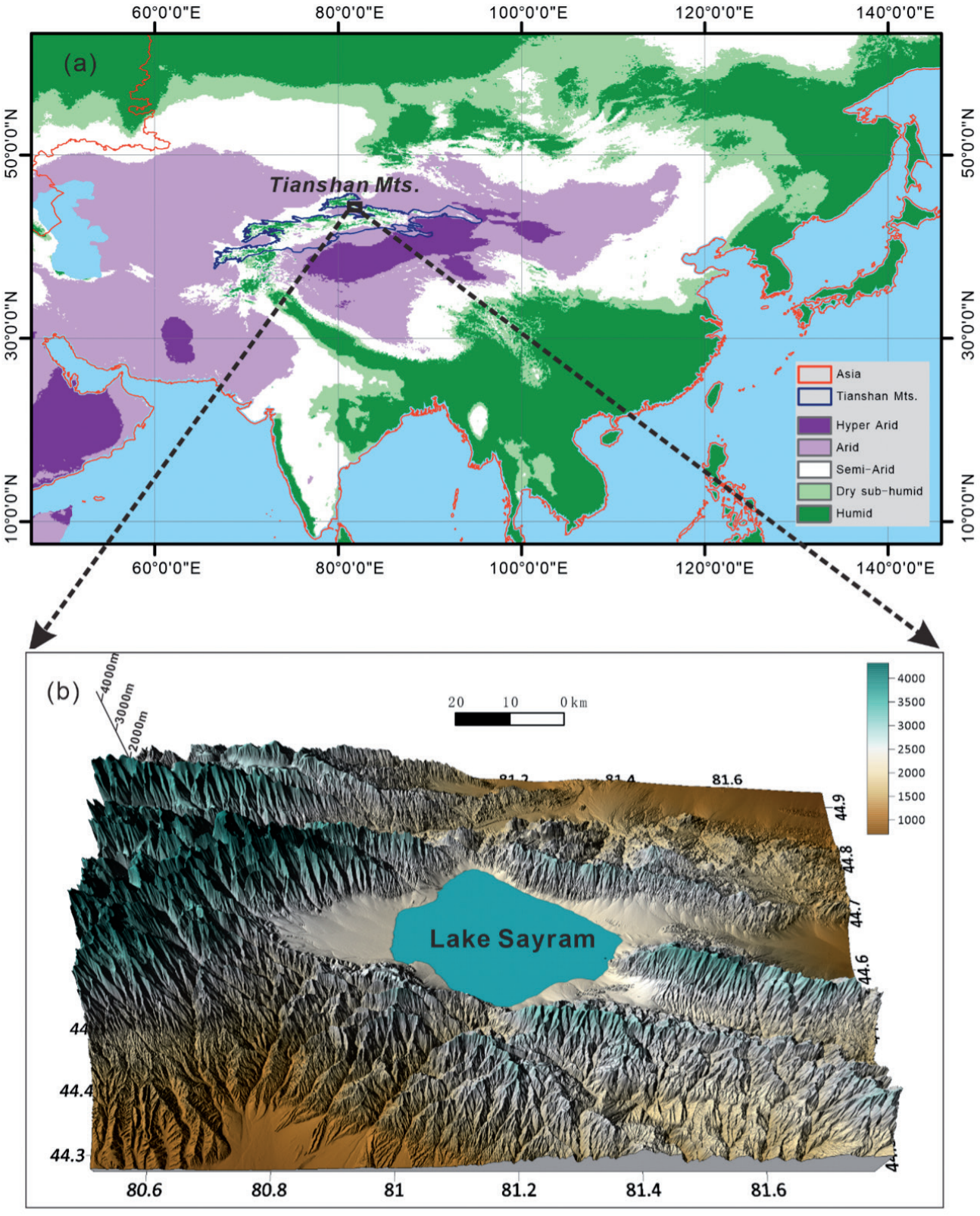

Fig 1. a) Location of Sayram Lake in the Tianshan Mountains (Mts) of Central Asia, with the background of the distribution of global arid lands (Zomer *et al.*, 2022); b) regional geomorphology of the SRTM 90m Digital Elevation database (Jarvis *et al.*, 2008).

Stable organic carbon isotopes ($\delta^{13}C$) were measured using a Finnegan MAT 251 Stable Isotope Mass Spectrometer (Thermo Finnigan, Waltham, MA, USA). A precise volume of the sample to be measured was transferred into a 100-mL beaker, followed by the addition of 5% dilute HCl. This process was performed to facilitate carbonate removal. After a 24-h reaction, distilled water was added to the beaker, which was left to stand overnight. The sample was then rinsed to neutrality by pumping out the upper layer of water, and the rinsing process was repeated four to five times. The specimen was combined with copper oxide, platinum wire, and copper wire inside a quartz amphora. Amalgamation was initially introduced into the vacuum line, followed by vacuum fusion sealing. The specimen was placed in a muffle furnace at 850°C for 2.5 h for oxidation. The produced carbon dioxide (CO_2) was collected and purified using a liquid nitrogen cold trap. CO_2 was then analyzed for carbon isotopes using a mass spectrometer (MS). The δ13C value of CO_2 was measured using an MAT-251 mass spectrometer. Notably, the analytical error of this process was consistently maintained below 0.05‰. The results were expressed in terms of PDB standards. Quality control: The precision of the carbon isotope analysis of national standard furnace black (GBW04407) was determined to be better than ±0.1‰. A Delta Plus stable isotope mass spectrometer (Thermo Finnigan) was used to analyze the organic nitrogen isotopes ($\delta^{15}N$).The EA-IRMS online system was used to oxidize, reduce, and convert the nitrogen in the samples to nitrogen gas, which was subsequently direct-

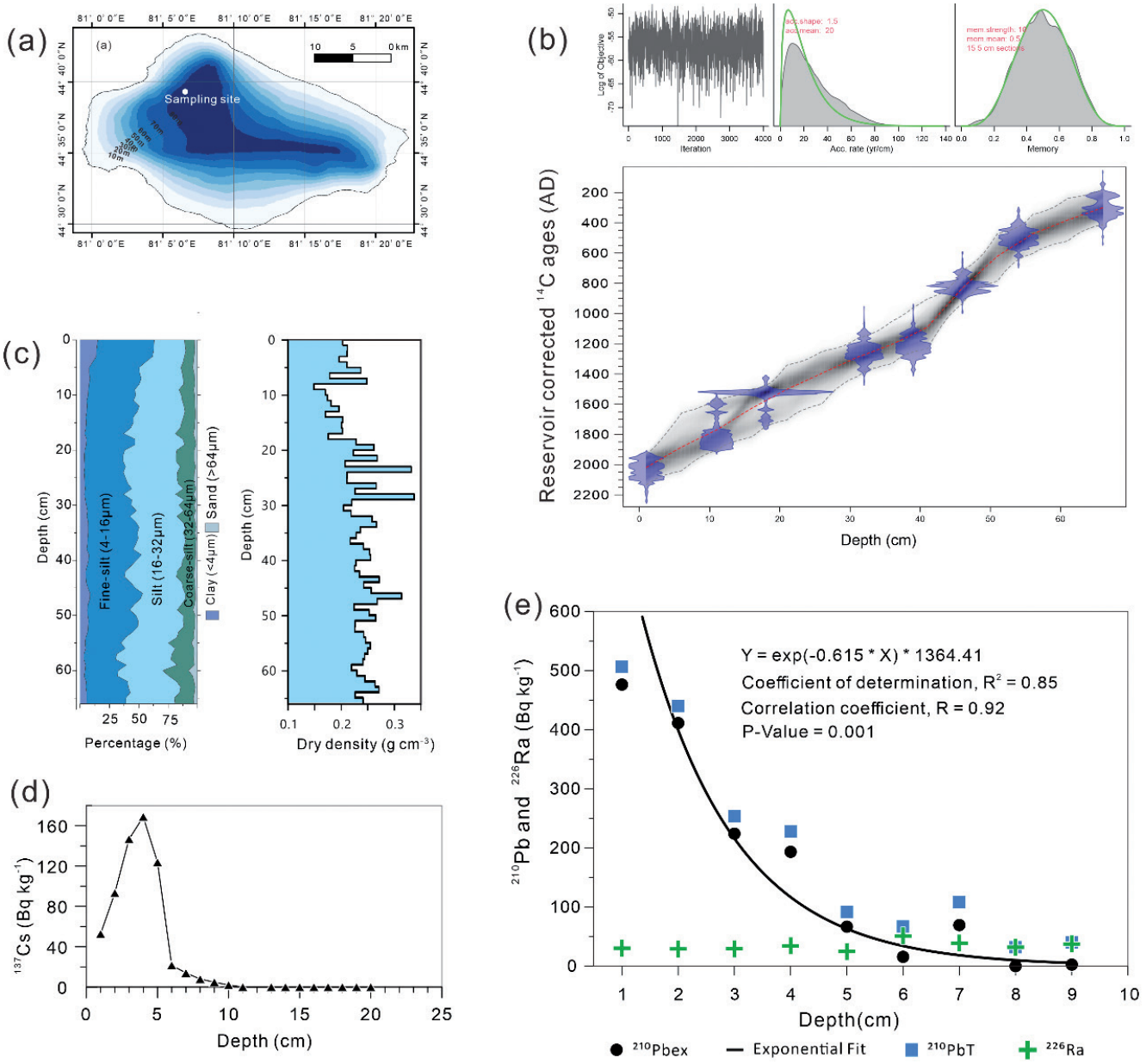

Fig. 2. a) Sediment core sampling site in Sayram Lake; b) age-depth model construction; c) core sediment grain size distribution and dry density across sediment core layers; d) specific activities of ^{137}Cs; e) specific activities of excess ^{210}Pb (^{210}Pbex), ^{226}Ra, and total ^{210}Pb (^{210}PbT).

ed to the mass spectrometer for nitrogen isotope analysis. Quality control: the analytical accuracy of the international standard IAEA-NO_3 (KNO_3) was greater than ±0.3‰ for $\delta^{15}N$.

The n-alkanes were analyzed using a GC/MS system (7890A/5975C; Agilent Technologies, Santa Clara, CA, USA) with a DB-5ms Ultra Inert column (30 m × 0.25 mm × 0.25 mm; Agilent Technologies) for chromatographic separation of the samples. The samples were then dried, ground, and passed through a 200-mesh sieve. A soil sample weighing 2 g was added to a dichloromethane: methanol solution (9:1) and sonicated for 30 min. The mixture was filtered, and the process was repeated thrice. The addition of an appropriate amount of copper wire to the solution was necessary to remove sulfur from the sample. Following this step, the sample underwent nitrogen blowdown and was left to dry completely. The sample was dissolved in a minimal amount of n-hexane, transferred to a silica gel column for filtration, and eluted from the column using n-hexane. The samples were then left to stand and air dried. The sample was subsequently stabilized using 200-microliter toluene solution and measured using the designated apparatus. Quality control measures involved the use of known concentrations of n-alkane standard solutions during machine testing and repetition of sample determinations. The resultant relative error was consistently maintained at below 10%.

Data processing and statistical methods

The burial flux of organic carbon quantifies the organic carbon buried per unit area and time and is calculated as OCBR = OCD × S × 10^4, where OCD = ρ_{dry} × TOC. Where OCAR represents the organic carbon burial flux. For ease of regional comparison, the units were expressed as g m^{-2} a^{-1}. Organic carbon density (OCD) indicates the absolute amount of organic carbon in a specific layer unit volume (g cm^{-3}). The sedimentation rate (S) was measured in cm a^{-1}, and the total organic carbon (TOC) content was expressed as a percentage. ρ_{dry}, which represents the mass of dry sediment per unit volume (g cm^{-3}), was calculated as ρ_{dry} = T/V. Here, T denotes the dry weight of the sediment at various depths (g), and V is the corresponding original sediment volume (cm^3).

Continuous wavelet analysis, implemented using the Python package "easyclimate" (https://zenodo.org/doi/10.5281/zenodo.10279567), has been extensively used to analyze the periodicity of time-series data (Lorenzo-Lacruz *et al.*, 2022; Wang *et al.*, 2022). This study utilized cross-wavelet transform (XWT) and wavelet coherence (WTC) analyses to examine the multiscale dependency between the two variables using the Python package "pyleoclim" (Khider *et al.*, 2022). Cross-wavelet analysis combines the advantages of wavelet transform in time-frequency analysis, enabling the simultaneous examination of the relationship between two time-series variables in the time and frequency domains (Liu *et al.*, 2024; Zhou *et al.*, 2022). It decomposes time series into different frequency scales through wavelet transform and then analyzes the correlation, phase relationship, *etc*., between variables at each scale, thereby revealing the dependency between variables at different time scales.

The mutation, seasonality, and trend Bayesian Estimator (BEAST) algorithm (Zhao *et al.*, 2019) was used for detection based on time-series information. Bayesian change point analysis in the R package «Rbeast» was used to identify possible change points and estimate their occurrence probabilities.

RESULTS

Age-depth model in sedimentology

The radiocarbon age of the top 1 cm layer was 2210 ± 30 BP (uncorrected for the $\delta^{13}C$ isotope fractionation). The underlying layers at 11 cm, 18 cm, 32 cm, 39 cm, 46 cm, 54 cm, and 66 cm depth yielded ages of 2410 ± 30 BP, 2600 ± 30 BP, 2880 ± 30 BP, 2910 ± 30 BP, 3240 ± 30 BP, 3510 ± 30 BP, and 3650 ± 30 BP, respectively (Tab. 1). By comparing the age of the 0-1 cm layer with the sampling time of 2023 AD, a significant carbon pool age was found. This carbon reservoir age was then applied to all sedimentary layers to establish a complete chronological framework for the Sayram Lake SLM core. The sedimentary core, extending to a depth of 65-66 cm, dates back to approximately 285 AD, providing a comprehensive record of climate and environmental changes in the Tianshan region over the past 1700 years (Fig. 2b).

To further validate the radiocarbon-based chronology, additional dating analyses were performed. The specific activity of ^{137}Cs was measured, and the variation curve exhibited a peak value of 168.80 Bq kg^{-1} at a depth of 4 cm. According to relevant studies, the peak in western China corresponds to the global nuclear testing peak in 1963-1964 AD (Lan *et al.*, 2020a). Radiocarbon dating of carbon reservoir-calibrated sediments from Sayram Lake indicated that the 4 cm layer dates to 1950 AD, and the 3 cm layer to 1973 AD, reflecting a relative consistency between the ^{137}Cs and ^{14}C ages. However, the ^{137}Cs activity at a depth of 10 cm was 2.0 Bq kg^{-1} (Fig. 2d). If this layer was independently dated to 1954 AD, it would have significantly diverged from the ^{14}C age of 1847 AD. Nonetheless, the analysis suggests a more probable explanation: vertical migration of ^{137}Cs could cause significant discrepancies in the dating of the layers where it appears, except for the maximum ^{137}Cs value. The activities of total ^{210}Pb (^{210}PbT) and ^{226}Ra are shown in Fig. 2e, and the excess

Tab. 1. Parameter table for the rbacon package with calibration curve for ^{14}C dates: cc=1 for IntCal20 (northern hemisphere terrestrial).

ID	Age	Error	Depth	cc
SS1	2210	30	1	1
S11	2410	30	11	1
S18	2600	30	18	1
S32	2880	30	32	1
S39	2910	30	39	1
S46	3240	30	46	1
S54	3510	30	54	1
S66	3650	30	66	1

^{210}Pb activity (^{210}Pbex=^{210}PbT-^{226}Ra) exhibited an approximately exponentially decreasing trend with depth. Based on the exponential distribution of excess ^{210}Pb specific activity (Fig. 2e), the age of the 9 cm layer was estimated to be approximately 1845 AD. This is consistent with the median age of 9 cm obtained from ^{14}C dating (1847 AD), further supporting the reliability of ^{14}C ages. However, a notable difference exists between the peak ages of 1944 AD for ^{210}Pb and ^{137}Cs at 4 cm depth, indicating that a comprehensive analytical comparison of the age-depth model is necessary. Nevertheless, overall, the peak age of ^{137}Cs and depth-balanced age of ^{210}Pb were more consistent with the ^{14}C age.

Organic proxy indicators, grain size and dry density for Sayram lake sediments

Fig. 2c illustrates the variations in clay (<4 μm), fine silt (4-16 μm), medium silt (16-32 μm), coarse silt (32-64 μm), and sand (>64 μm) within the sedimentary core. The clay content (<4 μm) ranges from approximately 3.35% to 15.21%. Generally, it showed a decreasing trend with increasing depth, especially at shallower depths (0-10 cm), where the decline was more pronounced. Subsequently, it fluctuated at different depths, but remained relatively low overall. The fine silt content (4-16 μm) ranged from approximately 26.88% to 48.7%. The content of medium silt (16-32 μm) ranged from 35.69% to 47.09%, and the fluctuation was relatively small, showing no obvious regularity at different depths and remaining within a relatively narrow range. The content range of coarse silt (32-64 μm) was approximately 7.71-19.67%, and it fluctuated to some extent with depth. It remains relatively stable at shallow depths. However, the fluctuation amplitude increased with depth, and the content was relatively high at certain depths. The sand content range (>64 μm) was 0.97%–7.48%; the overall content was relatively low. No obvious change in the trend was observed during the depth variation process, and the content fluctuations were relatively large. The density values fluctuated significantly at the different depths. For instance, at a depth of 24 cm, the density was relatively high, reaching approximately 0.332 g cm^{-3}, whereas at a depth of 9 cm, it was relatively low at approximately 0.149 g cm^{-3} (Fig. 2c).

Fig. 3 shows that the TOC content ranged from 2.59% to 4.43%, with an average of 3.41%. During certain periods, such as between

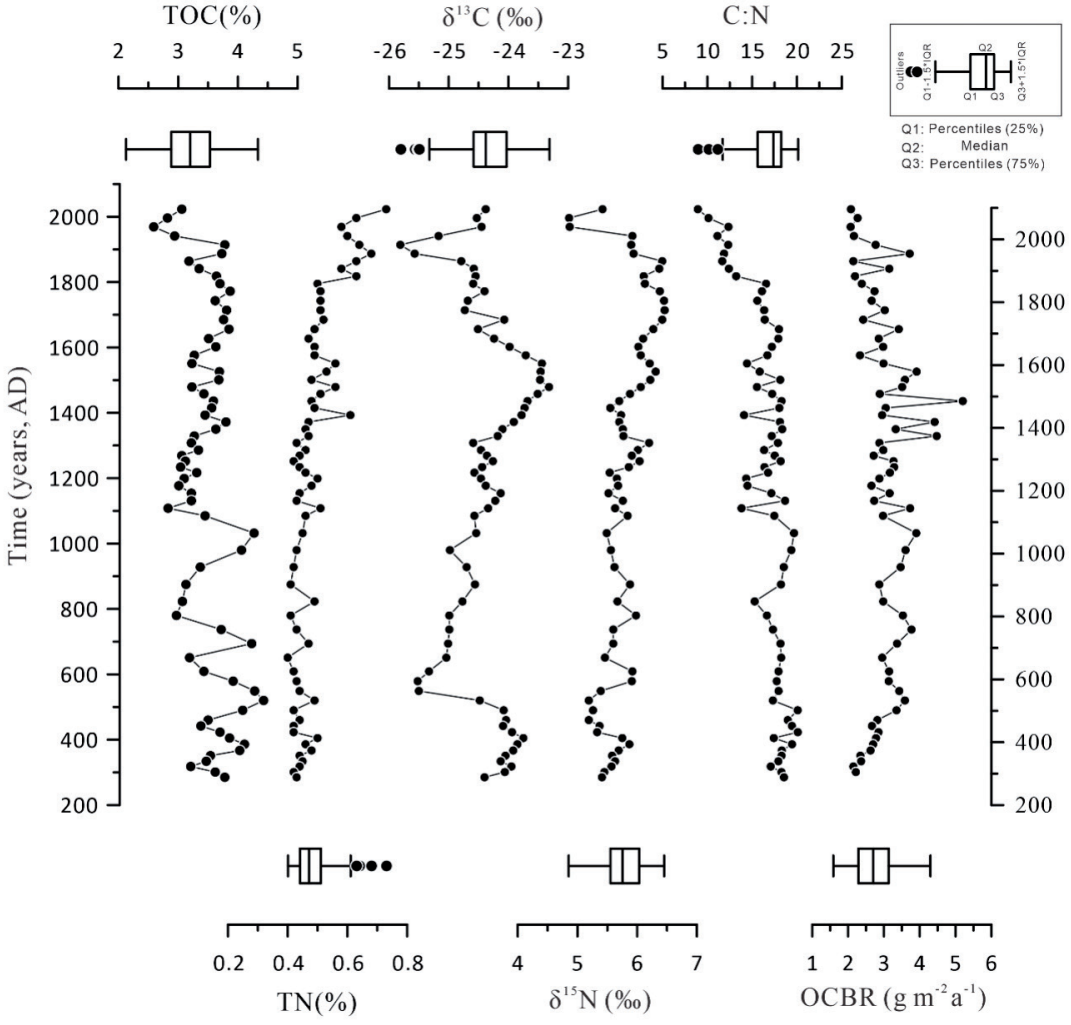

Fig. 3. Organic proxy indicators, such as total organic carbon (TOC), total nitrogen (TN), stable isotopes (δ^{13}C and δ^{15}N), and carbon-to-nitrogen molar ratio (C:N) in the SLM core sediment of Sayram Lake, along with the organic carbon burial rate (OCBR) across various periods.

1880 and 1910, there was a relatively high peak followed by a decline. The total nitrogen (TN) content varied between 0.41% and 0.73%, with an average of approximately 0.49%. $\delta^{13}C$ values range from −25.81‰ to −23.32‰ (mean −24.37‰), while $\delta^{16}N$ ranges from 4.86‰ to 6.46‰ (mean 5.72‰). No clear long-term covariation was observed between $\delta^{13}C$ and $\delta^{16}N$. The average carbon burial rate was approximately 3.02 g m^{-2} a^{-1}, ranging from a minimum of 2.07 g m^{-2} a^{-1} to a maximum of 5.20 g m^{-2} a^{-1}.

The Bayesian Estimation of Abrupt, Seasonal, and Trend (BEAST) algorithm identified two trend change points at 450AD and 1500 AD by dividing the record into three stages: before 450 AD (Stage I), 450-1500 AD (Stage II), and after 1500 AD (Stage III) (Fig. 4a). Wavelet power spectrum analysis of organic carbon burial density revealed a dominant periodicity in the 40-90-year band, with a peak at approximately 60 years (Fig. 4b). This periodic signal persisted throughout the past millennium, although its intensity exhibited interdecadal variations, with the strongest expression between 1300 and 1500 AD. The cone of influence (COI) and 95% confidence contours are indicated by the dashed and solid black lines, respectively.

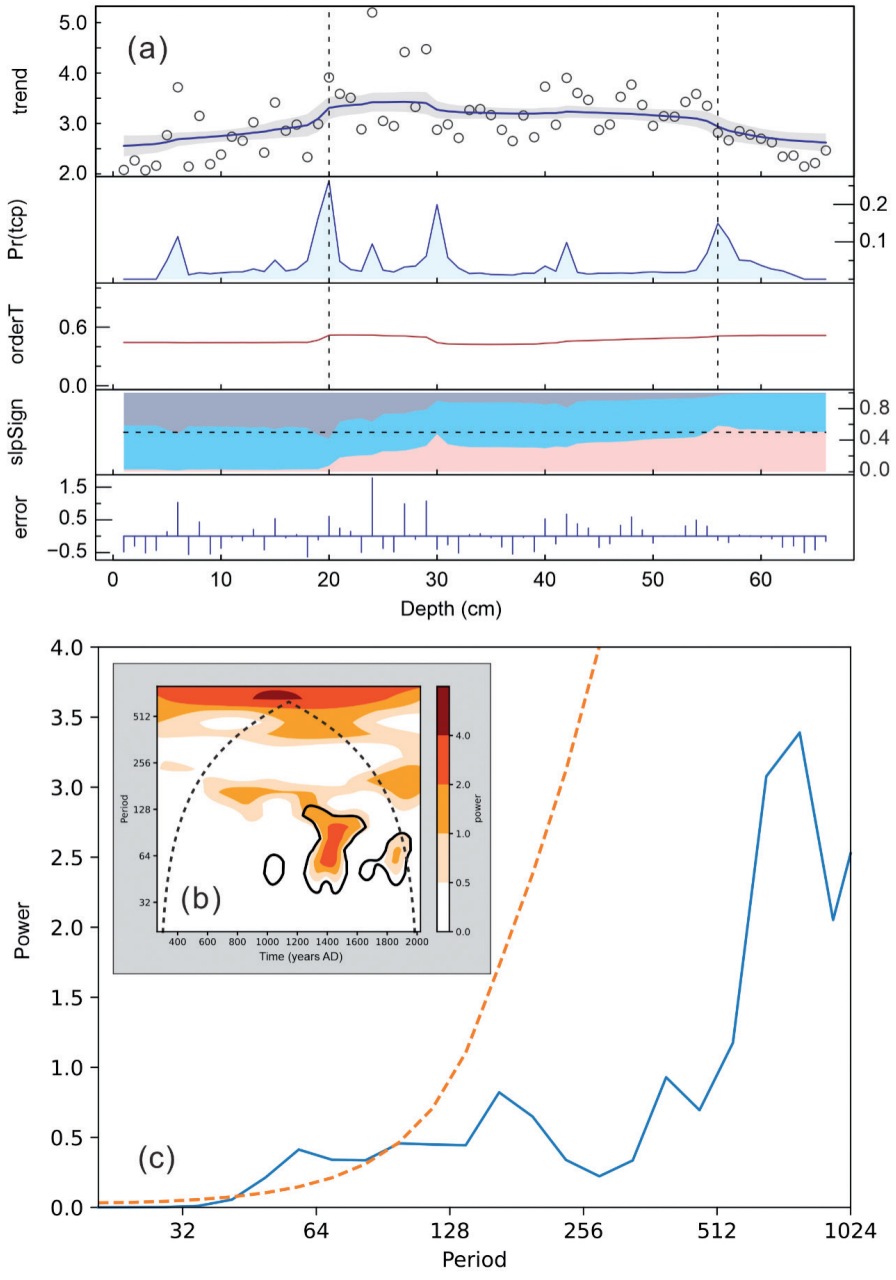

Fig. 4. Bayesian changepoint detection and time series decomposition (BEAST) of carbon burial density (a) complemented by a continuous wavelet plot (b) and plotting of the global wavelet spectrum (c) for carbon burial influx over time. The 40-90-year period band dominates, peaking at ~60 years (95% confidence, dashed line in panel c), with the strongest wavelet power between 1300 and 1500 AD (b). The black contours in panel b denote the 95% significance level, and the COI is shown by the dashed line.

Source apportionment of organic carbon based on n-alkanes

Although the simple linear correlation between TOC and TN was weak, wavelet coherence analysis revealed a significant multi-time-scale interdependence between the two variables, with most periodic regions exhibiting an anti-phase (negative) relationship (Fig. 5).Through the wavelet coherence map, the most significant coherence period was observed to be 20-100 years (Fig. 5). The good coherence among the signals was further demonstrated by the time series plotted in Fig. 5. During 260-600 AD, 1000-1200 AD, and 1350-1600 AD, the TOC and total nitrogen showed a relatively obvious reverse change on a 20-100-year cycle. This may reflect the variations in the proportions of terrestrial and aquatic biological sources.

Generally, the C:N ratio of vascular land plants is relatively high, usually between 20 and 30 or even higher (Meyers, 1994). Aquatic organisms, such as phytoplankton, zooplankton, and aquatic plants, typically exhibit low C:N ratios ranging from 4 to 10

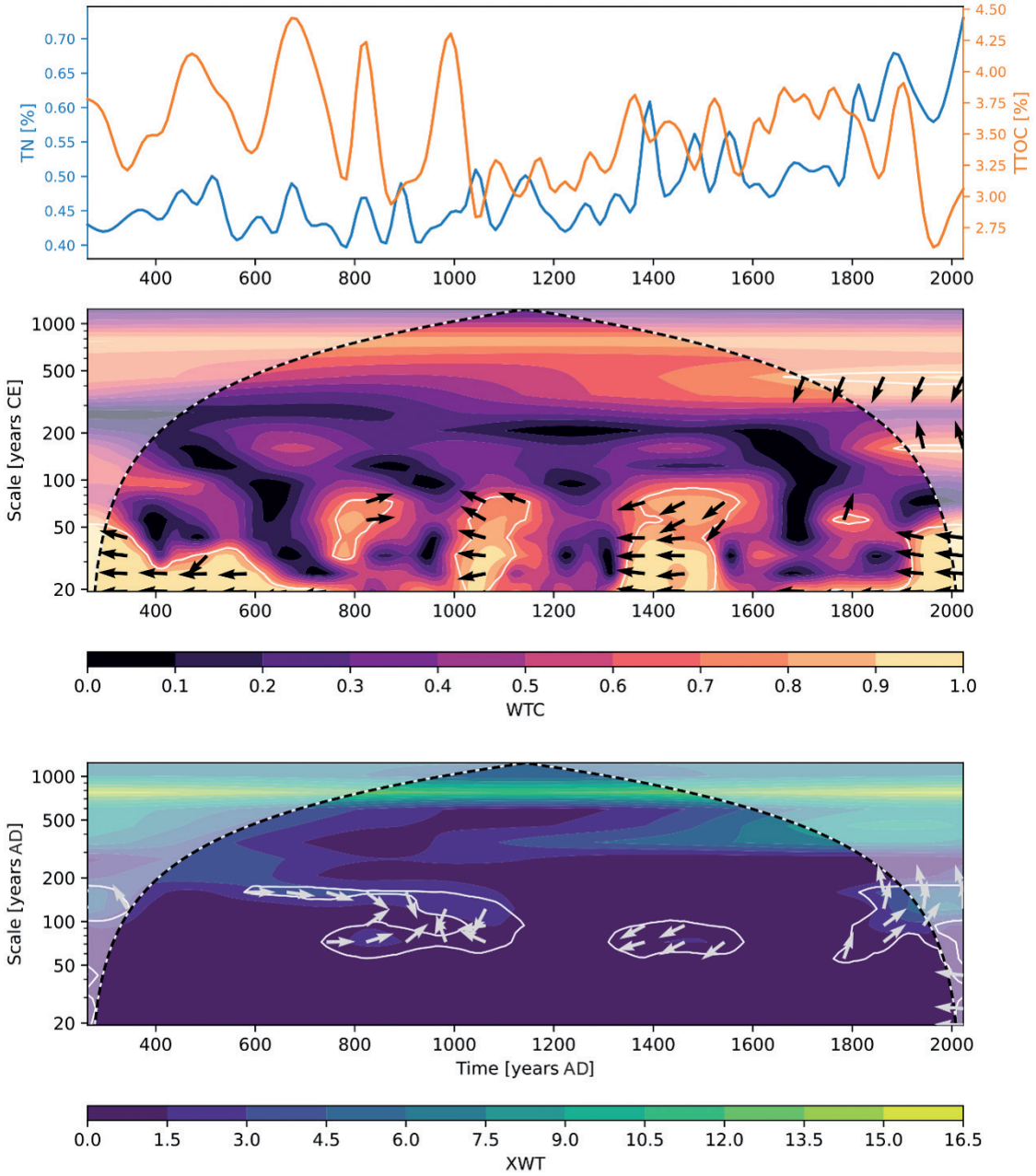

Fig. 5. Wavelet coherence (WTC) and cross-wavelet transform (XWT) plots between TN and TOC. Regions enclosed by white contours pass the 95% significance test, representing significant periodicities in the time-series. In the WTC plot, the color intensity reflects the strength of coherence, and the arrows indicate phase relationships: rightward arrows suggest in-phase behavior, whereas leftward arrows indicate anti-phase behavior.

(Meyers, 1997). This ratio is a common metric for differentiating between algal and terrestrial plant sources of sedimentary organic matter in aquatic environments, such as lakes and coastal areas (Douglas *et al.*, 2022; Yuan *et al.*, 2020; Zhao *et al.*, 2015). The observed mean C:N ratio was 16.49, with values ranging from 8.93 to 20.09. Therefore, terrestrial organic matter accounted for a relatively large proportion of the sediment in Sayram Lake.

Research indicates that long-chain n-alkanes (n-C_{27} to n-C_{35}) with a predominance of odd carbon numbers (n-C_{27}, n-C_{29}, and n-C_{31}) are primarily derived from terrestrial higher plants. In contrast, short-chain n-alkanes (n-C_{15} to n-C_{21}) originate from aquatic algae and planktonic bacteria, whereas medium-chain n-alkanes (n-C_{23} to n-C_{25}) originate mainly from large aquatic plants (da Silva *et al.*, 2008; Meyers, 1997). Different n-alkane carbon chain lengths are associated with distinct biological sources (Lin *et al.*, 2008) with algae and photosynthetic bacteria predominantly utilizing nC_{15}, nC_{17}, and nC_{19} alkanes (Cranwell *et al.*, 1987).Submerged and floating plants generally exhibit elevated n-C_{21}, n-C_{23}, and n-C_{25} alkane levels (Ficken *et al.*, 2000).Terrestrial vascular plants exhibit relatively high proportions of n-C_{27}, n-C_{29}, and n-C_{31} alkanes in their cuticular wax (Xiao *et al.*, 2025; Zheng *et al.*, 2009). This study utilized relevant research to comparatively analyze different sources (Fig. 6): C_{15}, C_{17}, and C_{19} as sources of algae and photosynthetic bacteria; C_{21}, C_{23}, and C_{25} as sources of submerged and floating

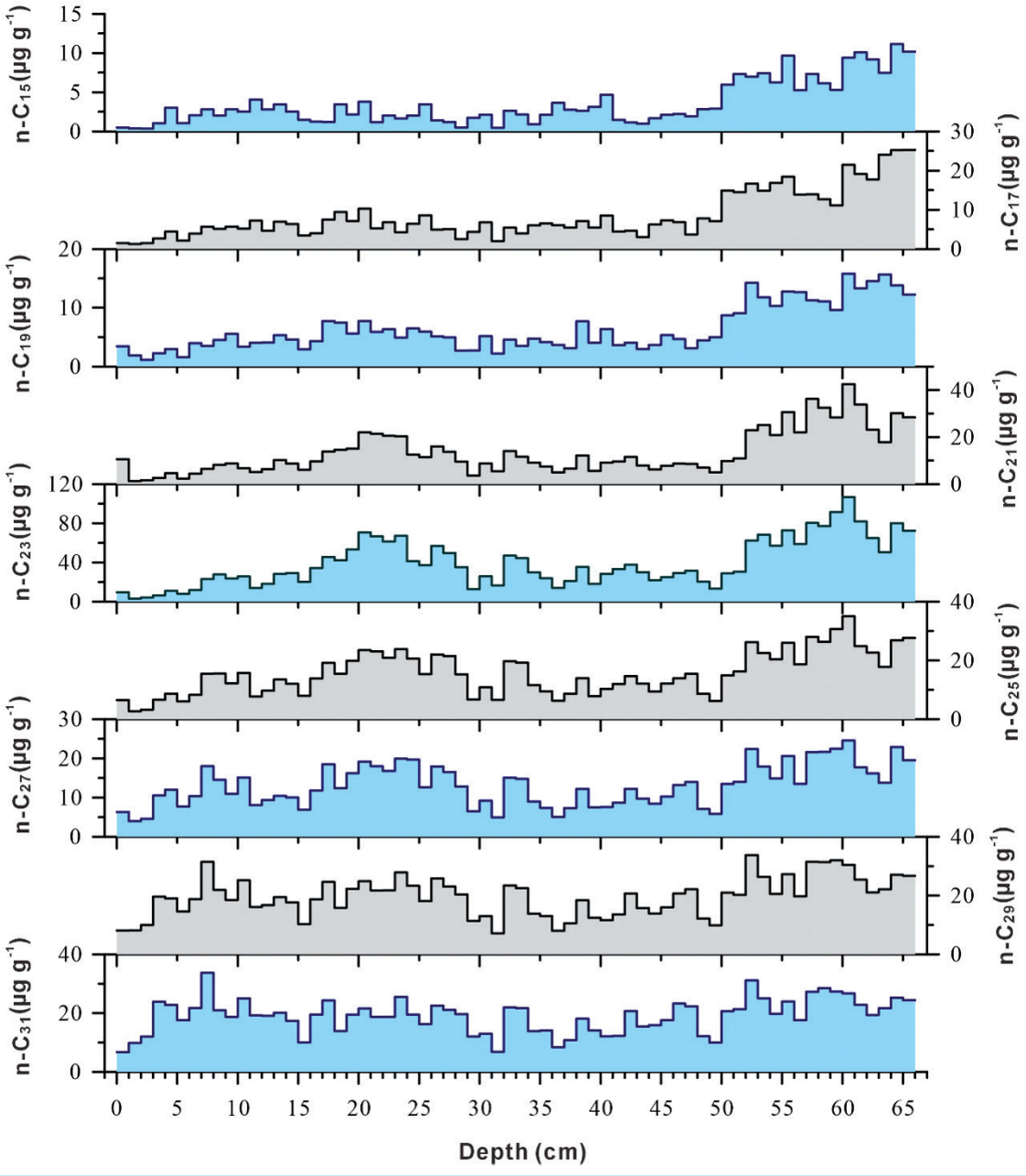

Fig. 6. The variation of C_{15}~C_{31} n-alkane content with depth.

plants; and C_{27}, C_{29}, and C_{31} as sources of terrestrial higher plants (Lin *et al.*, 2008; Pu *et al.*, 2009), and the contribution from the source of terrestrial higher plants was calculated.

DISCUSSION

Responses of organic carbon density to the sedimentary texture

It is generally acknowledged that clay (<4 μm) and fine silt (4-16 μm) enhance organic carbon adsorption and preservation because of their large specific surface area and surface charge, which typically show a positive correlation with organic carbon content (Hur *et al.*, 2009; Kennedy *et al.*, 2014; Yu *et al.*, 2009). Carbon burial in Sayram Lake sediments showed a negative correlation with clay (<4 μm) and fine silt (4-16 μm) (Fig. 7), suggesting differences from the conventional mineral protection mechanism (Hemingway *et al.*, 2019), complicating the traditional understanding of the relationship between carbon burial and grain size. In addition, organic carbon density was positively correlated with medium (16–32 μm) and coarse silt (32-64 μm), suggesting that these grain sizes are pivotal in enhancing carbon burial in the sedimentary environment of Sayram Lake. This phenomenon, which differs from the common relationship between grain size and organic carbon content, reflects the hydrodynamic conditions, material sources, biological activities, and chemical conditions that may exhibit special features. These features result in a specific relationship between the grain size and organic carbon density.

Responses of OCBR to regional environmental change

Major climate oscillations, such as the El Niño-Southern Oscillation (ENSO), North Atlantic Oscillation (NAO), and Pacific Decadal Oscillation (PDO), significantly regulate the multidecadal

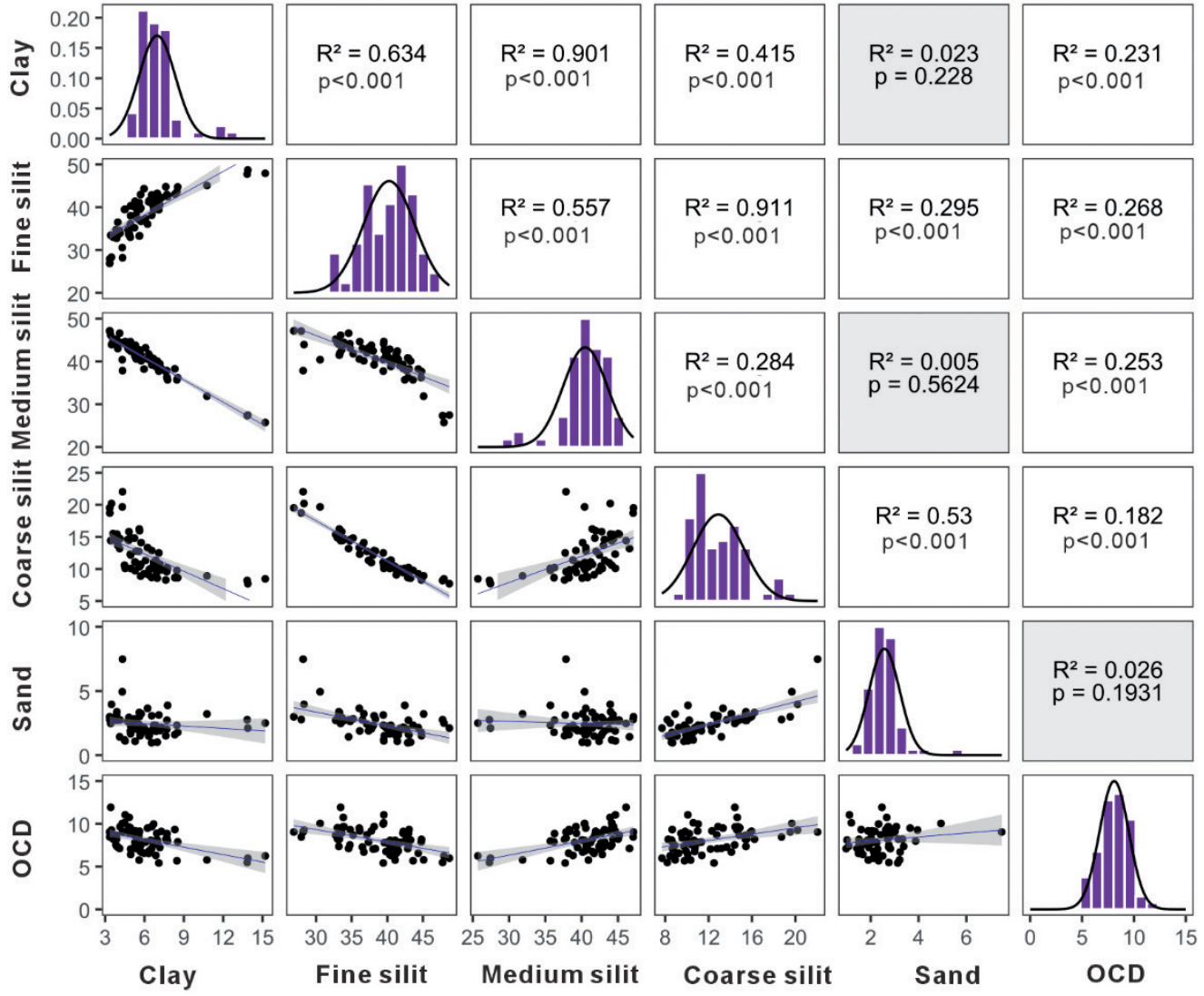

Fig. 7. The relationship between organic carbon density (OCD, kg m^{-3}) and grain size was expressed as a linear correlation.

variability of global and regional climates by influencing atmospheric and oceanic circulation (Årthun *et al.*, 2021; Power *et al.*, 2021). Some studies have indicated that atmospheric oscillation indices exhibit a significant 50-year correlation with solar radiation forcing, suggesting that external factors, such as solar radiation and volcanic activity, have notably influenced the 50-year variability of atmospheric oscillations over the past millennium (Man and Zhou, 2011). The carbon burial flux in the sediments of Sayram Lake exhibits significant decadal variability. A prominent power peak was observed within the 40-90-year period range, with the strongest signal at approximately the 60-year period. This pattern may be influenced by external forcing factors such as atmospheric oscillation indices.

In paleoclimatic research, the study of the characteristics and patterns of climate and environmental change over the past thousand years has always been a focus of academic attention (He *et al.*, 2025; White, 2025; Yu *et al.*, 2023). Notable climate events during this timeframe include the Medieval Warm Period, Little Ice Age, and Current Warm Period (Ding *et al.*, 2023; Mao *et al.*, 2023; Shi *et al.*, 2021). Research on sediment in the Sayram Lake Basin, a sub-basin of the Ebinur Lake Basin, indicates notable climatic and environmental changes during the Little Ice Age (~AD 1400-1750) and the Medieval Warm Period (~AD 1100-1300) (Ma *et al.*, 2011). The graph shows that the variation characteristics of carbon burial in Sayram Lake generally reflect the trend of temperature changes and were not a humidity response pattern over the past millennium (Fig. 8).

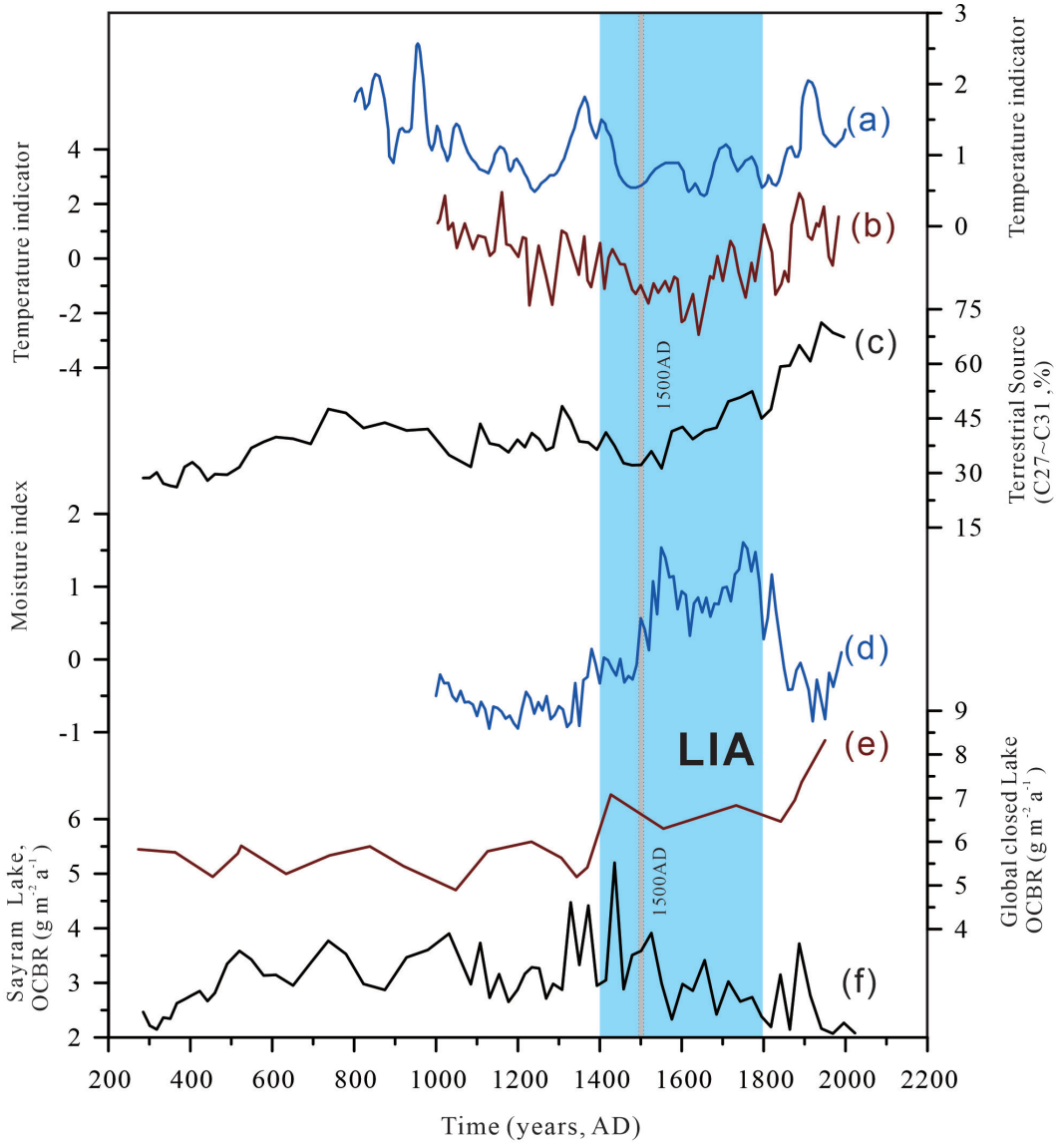

Fig. 8. Comparison of carbon burial and contribution of terrigenous organic carbon to regional environments. a) Temperature variations in tree-ring width chronologies in the Tianshan region of Kirghizia (Esper *et al.*, 2003); b) a millennium-long Central Asian temperature record synthesized from tree-ring data in the Karakorum and Tianshan Mountains (Yang *et al.*, 2009); c) a portion of terrestrial sources in organic carbon burial in Sayram Lake sediments; d) Holocene moisture changes in arid central Asia (Chen *et al.*, 2008); e) carbon sequestration in global inland basin lake sediments (Li *et al.*, 2025); f) organic carbon burial flux in Lake Sayram.

In arid regions, moisture primarily limits terrestrial vegetation growth, whereas temperature influences vegetation type and productivity by affecting evapotranspiration, the length of the growing season, and other physiological processes. However, the proportion of carbon buried in Sayram Lake sediments derived from terrestrial plants has a certain response relationship with temperature changes (Fig. 8). Cold conditions shorten the plant growing season and significantly reduce terrestrial organic matter input into lakes. Research on Sayram Lake showed that before 1500 AD (see the change point in the BEAST results), the proportion of terrestrial plant sources showed a relatively weak increasing trend and remained stable. A stable source of terrestrial plants indicates that the structure and coverage of terrestrial plant communities within the Sayram Lake Basin are relatively stable. Sayram Lake may have its own regulatory mechanism that enables it to maintain a relatively stable source of aquatic plants, even when external conditions change. During the late Little Ice Age, although temperatures rose and terrestrial biological inputs increased post-1500 AD, the overall climate remained cold. This results in a shortened plant growth period and reduced primary productivity. The extended ice sheet period likely restricted aquatic plant growth and significantly reduced carbon burial during the Little Ice Age.

In comparison with the carbon burial in the sediments of global inland basin lakes (Li *et al.*, 2025) (Fig. 8), it was also shown that deep-water lakes in arid inland mountains have significant differences in the carbon burial flux of lake sediments. On the same timescale as the sediments of Sayram Lake, the average carbon burial flux of global inland basin lake sediments is 6.04 g m^{-2} a^{-1}, while the carbon burial flux of Sayram Lake sediments is only 3.02 g m^{-2} a^{-1}, which is half of the global average. In comparison, it was found that not considering deep-water lakes in the mountains may overestimate the global inland lake burial rate. Globally, the burial rate of organic carbon in sediments has notably increased since approximately 1400 AD. However, the organic carbon burial flux of the Sayram Lake sediments showed an overall decreasing trend.

Research on organic carbon burial and its sources in Sayram Lake sediments has revealed that deep-water lakes in arid mountain ecosystems have distinct carbon burial mechanisms. On the one hand, the correlation between carbon burial in sediments and fine-grained substances is not close. This relationship is of great significance for understanding the carbon sequestration mechanisms, reconstructing paleoenvironments, and evaluating the ecological functions of lakes. For most of the past millennium, prior to 1500 AD, the sources of organic carbon in lakes indicated stable mountain ecosystems. Moreover, changes in primary productivity or carbon sequestration in mountain ecosystems reflect differences in carbon sequestration mechanisms between mountain and global inland ecosystems. This also indicates that global-scale carbon sequestration research needs to consider the differences between the various types of ecosystems.

CONCLUSIONS

This study investigated the mechanisms controlling organic carbon burial in the deep-lake sediments of Sayram Lake in the mountainous area of the arid Tianshan region over the past millennium. An age-depth model of the sediment core was developed using radiocarbon dating, and numerical model decomposition was applied to analyze temporal variations in the organic carbon burial flux. The influence of the lake environmental system evolution and climate change on organic carbon burial was investigated using regional climate change data.

The carbon burial pattern in the Tianshan Mountains of Central Asia was established for the first time over the past millennia. Utilizing the Bayesian ensemble algorithm for change-point detection and time-series decomposition, along with the continuous wavelet transform and cross-wavelet methods, this study thoroughly examined the characteristics of organic carbon burial and proposed a methodological framework for analyzing carbon burial across various time scales.

This study found that organic carbon burial in Sayram Lake sediments was characterized by the coexistence of periodicity and stages. There was a significant power peak within the 40–90-year period range, with the strongest signal occurring at approximately the 60-year period. The carbon burial time series was segmented into three distinct stages: prior to 450 AD, it exhibited a low level with an upward trend; from 450 to 1500 AD, it showed a high level with a modest increase; and post-1500 AD, which reflected a low level with a downward trend.

The amount of carbon buried progressively declined from the Medieval Warm Period to the Little Ice Age. This shows a significant difference from the changing trend in the organic carbon burial fluxes in the sediments of global inland basin lakes. This study provides new data and insight into the carbon burial mechanisms of deep-water lakes in mountain ecosystems in arid regions.

References

Anderson NJ, Heathcote AJ, Engstrom DR, Contributors Gd, 2020. Anthropogenic alteration of nutrient supply increases the global freshwater carbon sink. Sci Adv 6:eaaw2145.

Årthun M, Wills RCJ, Johnson HL, Chafik L, Langehaug HR, 2021. Mechanisms of decadal North Atlantic climate variability and implications for the recent cold anomaly. J Clim 34:3421-3439.

Bar-On YM, Li X, O'Sullivan M, Wigneron J-P, Sitch S, Ciais P, et al., 2025. Recent gains in global terrestrial carbon stocks are mostly stored in nonliving pools. Science 387:1291-1295.

Bradley RS, Briffa KR, Cole J, Hughes MK, Osborn TJ, 2003. The climate of the last millennium, pp. 105-141. In: Alverson KD, Pedersen TF, Bradley RS (eds.), Paleoclimate, global change and the future. Springer.

Cai X, Li Z, Zhang H, Xu C, 2021. Vulnerability of glacier change in the Tianshan Mountains region of China. J Geogr Sci 31:1469–1489.

Chen F, Yu Z, Yang M, Ito E, Wang S, Madsen DB, et al., 2008. Holocene moisture evolution in arid central Asia and its out-of-phase relationship with Asian monsoon history. Quat Sci Rev 27:351-364.

Cheng J, Meng X, Zhang E, Jiang Q, Ni Z, Ji J, 2021. An early Holocene primary dolomite layer of abiotic origin in Lake Sayram, Central Asia. Geophys. Res Lett 48:e2021GL096309.

Cranwell P, Eglinton G, Robinson N, 1987. Lipids of aquatic organisms as potential contributors to lacustrine sediments - II. Org Geochem 11:513–527.

da Silva LSV, Piovano EL, Azevedo DdA, Aquino Neto FRd, 2008. Quantitative evaluation of sedimentary organic matter from

Laguna Mar Chiquita, Argentina. Org Geochem 39:450-464.
Ding G, Chen J, Lei Y, Lv F, Ma R, Chen S, et al., 2023. Precipitation variations in arid central Asia over past 2500 years: Possible effects of climate change on development of Silk Road civilization. Glob Planet Change 226:104142.
Douglas PMJ, Stratigopoulos E, Park S, Keenan B, 2022. Spatial differentiation of sediment organic matter isotopic composition and inferred sources in a temperate forest lake catchment. Chem Geo. 603:120887.
Einsele G, Yan J, Hinderer M, 2001. Atmospheric carbon burial in modern lake basins and its significance for the global carbon budget. Glob Planet Change 30:167-195.
Esper J, Shiyatov SG, Mazepa VS, Wilson RJS, Graybill DA, Funkhouser G, 2003. Temperature-sensitive Tien Shan tree ring chronologies show multi-centennial growth trends. Chem Geol 21:699-706.
Falkowski P, Scholes RJ, Boyle E, Canadell J, Canfield D, Elser J, et al., 2000. The global carbon cycle: a test of our knowledge of earth as a system. Science 290:291-296.
Fan M, Xu J, Chen Y, Li W, 2020. Simulating the precipitation in the data-scarce Tianshan Mountains, Northwest China based on the Earth system data products. Arab J Geosci 13:637.
Fang L, Chen L, Liu Y, Tao W, Zhang Z, Liu H, Tang Y, 2015. Planktonic and sedimentary bacterial diversity of Lake Sayram in summer. MicrobiologyOpen 4:814-825.
Fang N, Zeng Y, Ran L, Wang Z, Lu X, Wang Z, et al., 2023. Substantial role of check dams in sediment trapping and carbon sequestration on the Chinese Loess Plateau. Commun. Earth Environ 4:65.
Feng S, Ma L, Abuduwaili J, Liu W, Saparov G, Issanova G, 2021. Organic carbon burial in the Aral Sea of Central Asia. Appl. Sci.-Basel 11:7135.
Ficken KJ, Li B, Swain D, Eglinton G, 2000. An n-alkane proxy for the sedimentary input of submerged/floating freshwater aquatic macrophytes. Org Geochem 31:745-749.
Harris I, Osborn TJ, Jones P, Lister D, 2020. Version 4 of the CRU TS monthly high-resolution gridded multivariate climate dataset. Sci Data 7:109.
He F, Yang F, Wang Y, 2025. Reconstructing forest and grassland cover changes in China over the past millennium. Sci China-Earth Sci 68:94-110.
He Y, Yang Tb, Ji Q, Chen J, Zhao G, Shao Ww, 2015. Glacier variation in response to climate change in Chinese Tianshan Mountains from 1989 to 2012. J Mt Sc. 12:1189-1202.
Hemingway JD, Rothman DH, Grant KE, Rosengard SZ, Eglinton TI, Derry LA, Galy VV, 2019. Mineral protection regulates long-term global preservation of natural organic carbon. Nature 570:228-231.
Hu Y, Cai J, Bai J, Zhang W, Gong Y, Jiang X, et al., 2025. Regime shift of bacterial communities in lake ecosystems in the arid and semi-arid north-west of China: Evidence from the sedimentary archives. Ecol Indic 172:113306.
Hülse D, Arndt S, Wilson JD, Munhoven G, Ridgwell A, 2017. Understanding the causes and consequences of past marine carbon cycling variability through models. Earth-Sci Rev 171:349-382.
Hur J, Lee D-H, Shin H-S, 2009. Comparison of the structural, spectroscopic and phenanthrene binding characteristics of humic acids from soils and lake sediments. Org. Geochem. 40:1091-1099.
Jarvis A, Reuter H, Nelson A, Guevara E, 2008. Hole-filled seamless SRTM data V4, International Centre for Tropical Agriculture (CIAT). Available from: http://srtm.csi.cgiar.org
Jiang Q, Ji J, Shen J, Matsumoto R, Tong G, Qian P, et al., 2013. Holocene vegetational and climatic variation in westerly-dominated areas of Central Asia inferred from the Sayram Lake in northern Xinjiang, China. Sci China-Earth Sci 56:339-353.
Jiang Q, Jin D, Zheng J, Yang Y, 2019. Abrupt climate events recorded by Sayram Lake sediments since the last deglaciation. Quat Sci 39:952-963.
Jiang Q, Zheng J, Yang Y, Zhao W, Ning D, 2020. A persistently increasing precipitation trend through the Holocene in Northwest China recorded by black carbon $\delta^{13}C$ from Sayram Lake. Front Earth Sc. 8:228.
Jones PD, Osborn TJ, Briffa KR, 2001. The evolution of climate over the last millennium. Science 292:662-667.
Kennedy MJ, Löhr SC, Fraser SA, Baruch ET, 2014. Direct evidence for organic carbon preservation as clay-organic nanocomposites in a Devonian black shale; from deposition to diagenesis. Earth Planet Sci Lett 388:59-70.
Khider D, Emile-Geay J, Zhu F, James A, Landers J, Ratnakar V, Gil Y, 2022. Pyleoclim: Paleoclimate timeseries analysis and visualization with Python. Paleoceanography Paleoclimatology 37:e2022PA004509.
Lan J, Wang T, Chawchai S, Cheng P, Zhou Ke, Yu K, et al., 2020a. Time marker of 137Cs fallout maximum in lake sediments of Northwest China. Quat Sci Rev 241:106413.
Lan J, Xu H, Lang Y, Yu K, Zhou P, Kang S, et al., 2020b. Dramatic weakening of the East Asian summer monsoon in northern China during the transition from the Medieval Warm Period to the Little Ice Age. Geology 48:307-312.
Lan J, Xu H, Liu B, Sheng E, Zhao J, Yu K, 2015. A large carbon pool in lake sediments over the arid/semiarid region, NW China. Chin J Geochem 34:289-298.
Li Y, Zhang X, Zhang Z, Gao M, Xue Y, 2025. Global lake carbon burial from endorheic zones since the Last Glacial Maximum and the future projection. Innov Geosci 3:100132.
Lin X, Zhu L, Wang Y, Wang J, Xie M, Ju J, et al., 2008. Environmental changes reflected by n-alkanes of lake core in Nam Co on the Tibetan Plateau since 8.4 kaB.P. Chin Sci Bull 53:3051–3057.
Liu D, Wang X, Wang Z, Zhu J, Li C, 2024. Integrated nonstationary and uncertain analysis of coupled relationship of hydrological connectivity and water level in a highly fragmented wetland. J Environ Manage 360:121137.
Liu W, Ma L, Abuduwaili J, Issanova G, Saparov G, 2021. Sediment organic carbon sequestration of Balkhash Lake in Central Asia. Sustainability 13:9958.
Liu W, Wu J, Ma L, Zeng H, 2014. A 200-year sediment record of environmental change from Lake Sayram, Tianshan Mountains in China. GFF 136:548-555.
Lorenzo-Lacruz J, Morán-Tejeda E, Vicente-Serrano SM, Hannaford J, García C, Peña-Angulo D, Murphy C, 2022. Streamflow frequency changes across western Europe and interactions with North Atlantic atmospheric circulation patterns. Glob Planet Change 212:103797.
Luo J, He M, Chang H, Liu X, 2025. Organic geochemistry analysis to decipher temporal carbon variations in Lop Nur Salt Lake, China. Paleogeogr Paleoclimatol Paleoecol 661:112735.
Ma L, Wu J, Abuduwaili J, Liu W, 2015. Aeolian particle transport

inferred using a~ 150-year sediment record from Sayram Lake, arid northwest China. J Limnol 74:1208.
Ma L, Wu J, Yu H, Zeng H, Abuduwaili J, 2011. The Medieval Warm Period and the Little Ice Age from a sediment record of Lake Ebinur, northwest China. Boreas 40:518–524.
Man W, Zhou T, 2011. Forced response of atmospheric oscillations during the last millennium simulated by a climate system model. Chin Sci Bull 56:3042.
Mao X, Liu X, Feng S, Li J, Li X, Jiang G, Liu L, 2023. Solar activity dominated the multidecadal-to centennial-scale humidity oscillations during the Little Ice Age in arid central Asia. Catena 223:106935.
Mendonça R, Müller RA, Clow D, Verpoorter C, Raymond P, Tranvik LJ, Sobek S, 2017. Organic carbon burial in global lakes and reservoirs. Nat Commun 8:1694.
Meyers PA, 1994. Preservation of elemental and isotopic source identification of sedimentary organic matter. Chem Geol 114:289-302.
Meyers PA, 1997. Organic geochemical proxies of paleoceanographic, paleolimnologic, and paleoclimatic processes. Org Geochem 27:213-250.
Power S, Lengaigne M, Capotondi A, Khodri M, Vialard J, Jebri B, et al., 2021. Decadal climate variability in the tropical Pacific: Characteristics, causes, predictability, and prospects. Science 374:eaay9165.
Pu Y, Zhang H, Lei G, Chang F, Yang M, Huang X, 2009. n-alkane distribution coupled with organic carbon isotope composition in the shell bar section, Qarhan paleolake, Qaidam basin, NE Tibetan Plateau. Front Earth Sci 3:327-335.
Quanliang J, Xiaohua M, Zhichun L, Shuaidong L, Changchun H, Tao H, et al., 2024. New perspectives on organic carbon storage in lake sediments based on classified mineralization. Catena 237:107811.
Shao K, Ba T, Qin B, Chao J, Gao G, 2023a. The prevalence of Atribacteria affiliated with JS1 in the sediment core of Lake Sayram, the largest alpine lake, China. J Limnol 82:2152.
Shao K, Qin B, Chao J, Gao G, 2023b. Sediment bacteria in the alpine lake Sayram: vertical patterns in community composition. Microorganisms 11:2669.
Shao K, Zhang L, Ba T, Chao J, Gao G, 2023c. Bacterial community composition of the sediment in Sayram Lake, an alpine lake in the arid northwest of China. BMC Microbiol 23:47.
Shen B, Wu J, Jin M, 2018. Sedimentary polycyclic aromatic hydrocarbons record recent anthropogenic activities near high-elevation Lake Sayram, northwest China. Limnologica 71:62-67.
Shi F, Lu H, Guo Z, Yin Q, Wu H, Xu C, et al., 2021. The position of the current warm period in the context of the past 22,000 years of summer climate in China. Geophys. Res Lett 48:e2020GL091940.
Stallard RF, 1998. Terrestrial sedimentation and the carbon cycle: Coupling weathering and erosion to carbon burial. Glob Biogeochem Cycle 12:231-257.
Tranvik LJ, Downing JA, Cotner JB, Loiselle SA, Striegl RG, Ballatore TJ, et al., 2009. Lakes and reservoirs as regulators of carbon cycling and climate. Limnol Oceanogr 54:2298-2314.
Wang J, Shi B, Zhao E, Yuan Q, Chen X, 2022. The long-term spatial and temporal variations of sediment loads and their causes of the Yellow River Basin. Catena 209:105850.
Wang S, Zhang M, Li Z, Wang F, Li H, Li Y, Huang X, 2011. Glacier area variation and climate change in the Chinese Tianshan Mountains since 1960. J Geogr Sci 21:263-273.
White S, 2025. Climate Change in Global Environmental History. A Companion to Global Environmental History, pp. 361–374.
Wu J, Liu W, Zeng H, Ma L, Bai R, 2014. Water quantity and quality of six lakes in the arid Xinjiang Region, NW China. Environ Process 1:115–125.
Xiao B, Cheecham-Uhrich D, Eickmeyer DC, Kimpe LE, Prėskienis V, Kivilä EH, et al., 2025. Long chain n-alkanes in lake sediment track differences in adjacent land vegetation. Org Geochem 202:104934.
Xie Z, He J, Lü C, Zhang R, Zhou B, Mao H, et al., 2015. Organic carbon fractions and estimation of organic carbon storage in the lake sediments in Inner Mongolia Plateau, China. Environ Earth Sci 73:2169-2178.
Xu H, Lan J, Liu B, Sheng E, Yeager KM, 2013. Modern carbon burial in Lake Qinghai, China. Appl Geochem 39:150-155.
Yang B, Wang J, Bräuning A, Dong Z, Esper J, 2009. Late Holocene climatic and environmental changes in arid central Asia. Quat Int 194:68-78.
Yao Y, Lan J, Zhao J, Vachula RS, Xu H, Cai Y, et al., 2020. Abrupt freshening since the early Little Ice Age in Lake Sayram of arid central Asia inferred from an alkenone isomer proxy. Geophys Res Lett 47:e2020GL089257.
Yu B, Dong H, Jiang H, Lv G, Eberl D, Li S, Kim J, 2009. The role of clay minerals in the preservation of organic matter in sediments of Qinghai Lake, NW China. Clay Clay Min 57:213-226.
Yu S-Y, Li W-J, Zhou L, Yu X, Zhang Q, Shen Z, 2023. Human disturbances dominated the unprecedentedly high frequency of Yellow River flood over the last millennium. Sci Adv 9:eadf8576.
Yu Z, Wang X, Zhao C, Lan H, 2015. Carbon burial in Bosten Lake over the past century: Impacts of climate change and human activity. Chem Geol 419:132-141.
Yuan H, Tai Z, Li Q, Zhang F, 2020. Characterization and source identification of organic phosphorus in sediments of a hypereutrophic lake. Environ Pollut 257:113500.
Zeng H, Wu J, Liu W, 2014. Two-century sedimentary record of heavy metal pollution from Lake Sayram: A deep mountain lake in central Tianshan, China. Quat Int 321:125-131.
Zhang F, Yao S, Xue B, Lu X, Gui Z, 2017. Organic carbon burial in Chinese lakes over the past 150 years. Quat Int 438:94-103.
Zhao K, Wulder MA, Hu T, Bright R, Wu Q, Qin H, et al., 2019. Detecting change-point, trend, and seasonality in satellite time series data to track abrupt changes and nonlinear dynamics: A Bayesian ensemble algorithm. Remote Sens Environ 232:111181.
Zhao Y, Wu F, Fang X, Yang Y, 2015. Topsoil C/N ratios in the Qilian Mountains area: Implications for the use of subaqueous sediment C/N ratios in paleo-environmental reconstructions to indicate organic sources. Paleogeogr Paleoclimatol Paleoecol 426:1-9.
Zheng Y, Zhou W, Xie S, Yu X, 2009. A comparative study of n-alkane biomarker and pollen records: an example from southern China. Chin Sci Bull 54:1065-1072.
Zhou S, Long H, Chen W, Qiu C, Zhang C, Xing H, et al., 2025a. Temperature seasonality regulates organic carbon burial in lake. Nat Commun 16:1049.
Zhou Y, Xu J, Ye W, Wang K, Lu H, Tang X, et al., 2025b. Source identification of organic carbon in mountainous reservoirs

sediments using stable isotopes and n-alkanes. J Geophys Res-Biogeosci 130:e2024JG008323.

Zhou Z, Liu S, Ding Y, Fu Q, Wang Y, Cai H, Shi H, 2022. Assessing the responses of vegetation to meteorological drought and its influencing factors with partial wavelet coherence analysis. J Environ Manage 311:114879.

Zomer RJ, Xu J, Trabucco A, 2022. Version 3 of the global aridity index and potential evapotranspiration database. Sci Data 9:409.

Received: 18 April 2026; Accepted: 22 June 2026.

Edited by: Franco Tassi, *Department of Earth Sciences, University of Florence, Italy.*

Citation: Liu W, Wang J, Guo J, et al. Millennial reconstruction of organic carbon burial and n-alkane-based source identification in Sayram Lake, Xinjiang, China. *J Limnol 2026;85:2272*.

Contributions: Wen Liu, data curation; formal analysis; methodology; visualization; writing – original draft preparation. Jingyu Wang, formal analysis; writing – original draft preparation. Yanli Guo, investigation; visualization. Yizhen Li, investigation; methodology; visualization. Tao Zeng, investigation; Long Ma, conceptualization; funding acquisition; investigation; methodology; project administration; writing – review & editing.

Conflicts of interest: the authors declare no competing interests, and all authors confirm accuracy.

Funding: this study was supported by Tianshan Talent Training Program (2023TSYCCX0083), Natural Science Foundation of Xinjiang Uygur Autonomous Region (2023D01A07), and State Key Laboratory of Ecological Safety and Sustainable Development in Arid Lands (E455020801).

Availability of data: Data are available from the authors upon reasonable request.

Acknowledgements: the authors thank the journal editors and anonymous reviewers for their constructive comments and professional suggestions. The authors acknowledge the Sayram Lake Scenic Area Management Committee, Bortala Mongolian Autonomous Prefecture, Xinjiang Uygur Autonomous Region, for providing support and assistance during field investigation and sampling.